Astron. Astrophys. 318, 947–956 (1997)

ASTRONOMY
AND
ASTROPHYSICS

The photospheric dynamo

I. Physics of thin magnetic flux tubes

J.C. Hénoux[1] **and B.V. Somov**[2]

[1] Observatoire de Paris, DASOP-LPSH, URA2080, F-92195 Meudon Principal Cedex, France (henoux@mesiob.obspm.fr)
[2] Astronomical Institute of the Moscow State University, Universitetskii Prospekt 13, Moscow B-234, 119899, Russia

Received 8 January 1996 / Accepted 19 March 1996

Abstract. In a previous paper (Hénoux and Somov, 1991) it has been shown that, in an initially weak magnetic field, a radial inflow of neutrals can generate azimuthal DC currents, and that an azimuthal velocity field can create radial DC currents leading to the circulation of vertical currents. The effects of such azimuthal velocity field on the intensity and topology of electric currents flowing in thin magnetic flux tubes is now investigated in detail in this paper. Two systems of currents flowing in opposite direction are created connected at photospheric level by transverse currents. The electromagnetic forces produced by these currents play a significant rôle in the structure and dynamics of flux tubes. Even for moderate values of the azimuthal photospheric velocities, the currents created are strong enough to prevent by the pinch effect an opening of the flux tube with height; despite the decrease of the ambient gas pressure with height, the thin flux tube extends into the solar atmosphere above the temperature minimum region.

In the internal current shell, the rise from the photosphere of a partially ionized gas is found to have two main effects: (a) the upflow of this gas associated to a leak of neutrals across magnetic field lines leads to an increase of the ionization degree with altitude typical for the chromosphere, and brings above the temperature minimum region an energy flux comparable to the flux required for chromospheric heating, (b) the outflow of neutrals that takes place at the chromospheric level across magnetic field lines, and leads to ion-neutral separation, may explain the observed abundance anomalies in the corona by enhancing in the upper part of the tube the abundances of elements of low ionization potential.

Upward motions are also present between the two current systems outside the internal cylindrical current. Their velocity is high enough to lift the matter to an altitude characteristic of spicules.

Key words: Sun: magnetic fields; chromosphere

Send offprint requests to: J.C. Hénoux

1. Introduction

In the deep photosphere, particles are well coupled by collisions. That is why the physics of magnetic flux tubes is often described by the resistive one-fluid MHD approach. However a treatment of the atmosphere as an ensemble of three fluids (ions, electrons and neutrals) is necessary to give a clear physical insight on the mechanisms of current generation in these flux tubes. Moreover, higher in the solar atmosphere significant effects arise due to the density decrease that leads to a decoupling of motions of ions and neutrals, that cannot be described by the one-fluid approximation.

For an axially symmetrical magnetic field, the velocities of electrons, ions and neutrals in the photosphere have been found analytically in Hénoux and Somov (1991), referred as Paper 1 in what follows, by solving the equations describing the balance of horizontal forces. A quantitative model of the photospheric flux tube is obtained. Then a model of the chromospheric part of the flux tube is presented showing the effects of the electromagnetic and pressure forces generated by the current system. This model is still semi-quantitative. However, it allows us to relate the DC currents in flux tubes to the photospheric velocity field and demonstrates the significant rôle of these currents in the physics of flux tubes.

The plan of the paper is the following. In Sect. 2 we show that an influx of matter and angular momentum inside the flux tube at photospheric level generates azimuthal and radial current densities. In Sect. 3 the vertical electric current, which keeps the flux tube in a pinched state in the chromosphere, is computed together with the vertical current density profiles. We discuss the photospheric upflows generated by the electromagnetic forces inside the flux tube in Sect. 4. Vertical currents produce large effects at chromospheric heights; they are presented in Sect. 5. Next, we discuss in Sect. 6 three main consequences of the electromagnetic forces generated by DC currents flowing in the flux tube: coronal abundance anomalies, formation of chromospheres, and acceleration of spicules. Conclusions are given in Sect. 7.

2. DC electric current generation

In a non axially symmetrical geometry, electric currents can be generated in separatrices or separators of the coronal magnetic field, for example, by shear motions either parallel or perpendicular to the photospheric neutral line. For axially symmetrical magnetic fields, steady azimuthal motions can generate currents. In this case, two models of current generation are distinguished.

The first one assumes the plasma is fully ionized with infinite conductivity. Hence, the magnetic field is frozen and moves with the plasma. Consequently, the generation of an azimuthal component of the field, and subsequently of a current along the flux tube, requires a variation of the angular velocity ω in the azimuthal plasma velocity $V_\theta = r\,\omega$ along s, the flux tube length, i.e. $d\omega/ds \neq 0$ (see Ch. 11 in Somov (1994) for a review). The current density is just derived from Ampère's law, $\boldsymbol{j} = 1/\mu \nabla \times \mathbf{B}$. The most acceptable location for this mechanism is below the photosphere where the plasma kinetic energy dominates over the magnetic energy. This model is widely used to explain qualitatively the generation of currents by twisting the photospheric part of magnetic loops where both feet are anchored in the deep and dense photosphere. However, it is difficult to conceive how this mechanism could generate currents in open flux tubes where the rotation of the upper part of the structure cannot be controlled by the rarified upper atmosphere. Moreover, no steady-state situation is obtained since a continuous twisting of the lines of force in the very deep photosphere leads to a continuous increase of the azimuthal B_θ component of the field (Steinolfsen 1991).

In the second model presented in this paper, where currents are generated by azimuthal motions in a partially ionized atmosphere, the azimuthal velocities may be constant along the loop length. Since it is the relative azimuthal velocity between the magnetic field lines and the partially ionized atmosphere that generates currents, these currents can result either from azimuthal motions of the gas around a fixed magnetic field or from the rotation around the flux tube axis of the magnetic field imbedded in a static partially ionized atmosphere.

Assuming steady state, the azimuthal and radial components of the current density can be derived from the steady equation of fluid dynamics

$$\rho\,\mathbf{V}\,\nabla\mathbf{V} = \mathbf{F}\,. \tag{1}$$

The corresponding equation for the horizontal components of the forces and velocities, in a thin flux tube of constant cross section, leads to the following expressions for the azimuthal and radial current densities

$$j_\theta = \left(j_z\,B_\theta + \frac{\partial p}{\partial r}\right)\frac{1}{B_z}\,, \tag{2}$$

where the contribution of the terms of inertia is neglected, and

$$j_r = -\frac{\rho}{B_z}\,\frac{V_r}{r}\,\frac{\partial\,(rV_\theta)}{\partial r}\,. \tag{3}$$

Eq. (3) shows that radial current generation requires an influx of matter and angular momentum inside the flux tube. The radial current density cannot be computed without knowing the plasma radial velocity V_r.

3. Currents generated in a partially ionized medium

3.1. Basic equations

The solution of the equation of dynamics for the horizontal motions of a partially ionized plasma (Paper 1, see also Hénoux and Somov, 1993 and 1994) gives a set of four equations:

$$j_\theta = \left(j_z\,B_\theta + \frac{\partial p_n}{\partial r}\right)\frac{1}{B_z}\,, \tag{4}$$

$$j_r = -\frac{n_n\,m_n}{B_z}\,\frac{V_{r,n}}{r}\,\frac{\partial(rV_{\theta,n})}{\partial r}\,, \tag{5}$$

$$V_{r,n} = \frac{1}{2\mu\alpha_s}\left(\frac{\partial B_z^2}{\partial r}(1+\frac{\alpha_s}{\sigma B_z^2}) + \frac{\mu^2}{4\pi r^2}\,\frac{\partial J_z^2}{\partial r}\right) + \frac{j_r}{n_e e}, \tag{6}$$

$$r\,V_{\theta,n} = -\,n_n m_n V_{r,n}\left(\frac{1}{\alpha_s} + \frac{1}{B_z^2\,\sigma}\right)\frac{\partial\,(rV_{\theta,n})}{\partial r}\,. \tag{7}$$

Here σ is the electric conductivity and $\alpha_s = n_e(m_i\nu_{i,n}+m_e\nu_{e,n})$ where $\nu_{i,n}$ and $\nu_{e,n}$ are respectively the neutral-ion and neutral-electron collisional frequencies taken from Kubát and Karlický (1986). The equations (6) and (7) are derived in Appendix (Eqs. B.3 and C.1). The radial and vertical current densities are related by the particle conservation law

$$\frac{\partial j_z}{\partial z} = -\frac{1}{r}\,\frac{\partial\,(rj_r)}{\partial r}\,, \tag{8}$$

and we have the additional relations between variables

$$j_\theta = -\frac{1}{\mu}\frac{\partial B_z}{\partial r} \quad \text{and} \quad J_z = \int 2\pi\,r j_z\,dr.$$

The radial variation of the vertical component of the field was taken to be identical to the one that corresponds to null azimuthal velocities and to a linear dependence on radial distance of $V_{r,n}$ the neutral radial velocity. Then the set of Eqs. (4) to (7) was solved iteratively. Since J_z, the vertical electric current intensity, appears in Eq. (6), the current densities j_r and j_θ cannot be derived locally, i.e. independently of the contribution of the other atmospheric layers. A circuit model is necessary to relate the total current J_z to the current densities.

3.2. Electric current circuit

Every layer l acts as a current generator in a circuit that extends above and below this layer. Two main circuit models are possible. One where the flux tube is at the foot of a magnetic loop, and the circuit extends to the other foot of this loop. Another model where the flux tube opens and keeps its axial symmetry. In this case, currents transverse to the magnetic field are required in the upper coronal and lower convective part of the flux tube to close the circuit.

In all cases the contributions of every layer to the circuit regions placed above and below it are proportional to the inverse ratio of the resistances of these parts of the circuit. The use of the

parallel conductivity to estimate the resistance is valid for a loop type circuit and, as shown below, is still a good approximation in the case of an open flux-tube:
In the case of an open flux tube, the parallel and transverse resistances in the fully ionized coronal and convective parts of the circuit are related by

$$\frac{R_\perp}{R_\parallel} = \frac{\sigma_\parallel}{\sigma_\perp} \left(\frac{\Delta r}{L}\right)^2, \tag{9}$$

where L and Δr are the length of the flux tube and the radial distance between the two opposite cylindrical current channels. The transverse Hall conductivity $\sigma_\perp$ is equal to $\omega\tau/(1+\omega^2\tau^2)\ \sigma_\parallel$, where ω and τ are respectively the electron gyrofrequency and the ion-electron collisional time, and $\sigma_\parallel$ is the conductivity parallel to field lines. Consequently in the low density corona the ratio $\sigma_\parallel/\sigma_\perp$ is close to $\omega\tau$. For an electron density in the coronal part of the flux tube of 10^{10} cm^{-3} and a magnetic field of 100 G, the product $\omega\tau$ is $\approx 10^6$. Therefore, for a radial distance Δr between the two cylindrical shells of current of about 10 km, and over a length L of 10^4 km, the transverse and longitudinal resistances are equal. On the other hand, in the convective zone for a magnetic field of 100 G, at densities higher than about 10^{18} cm^{-3}, the conductivity is isotropic. Consequently, we estimated the resistance of the coronal and photospheric parts of an open flux tube by using $\sigma_\parallel$ for the conductivity.

The resistance of the part of the circuit respectively above and below a layer l are respectively

$$R_a = \int_l^N \sigma_\parallel^{-1} ds,$$

where the integration is made from the layer l to the uppest layer N of the VAL C atmospheric model (Vernazza *et al.* 1981) used and

$$R_b = \int_l^1 \sigma_\parallel^{-1} ds\,,$$

where the integration is made from the layer l to the lowest layer of the VAL C atmospheric model. Consequently the contributions $dj_z^{\,a}$ and $dj_z^{\,b}$ to the current flowing above or below every layer l are given by

$$dj_z^{\,a} = \left(\frac{\partial j_z}{\partial z}\right)_l \frac{R_b}{R_a+R_b}\, dz\,, \tag{10}$$

$$dj_z^{\,b} = \left(\frac{\partial j_z}{\partial z}\right)_l \frac{R_a}{R_a+R_b}\, dz\,. \tag{11}$$

The resulting current density in the layer k is

$$j_z = \sum_{l=k}^{l=N} dj_z^{\,a} - \sum_{l=1}^{l=k} dj_z^{\,b}\,, \tag{12}$$

and the total current $J_z = \int 2\pi\, r j_z\, dr$. Iterations are made between the two systems of Eqs (5) to (8) and (10) to (12). It is worth noticing that equation (5) shows that the lower B_z the higher the radial current density j_r must be, in order to generate a given breaking force. Consequently, the radial currents are generated in low vertical magnetic fields.

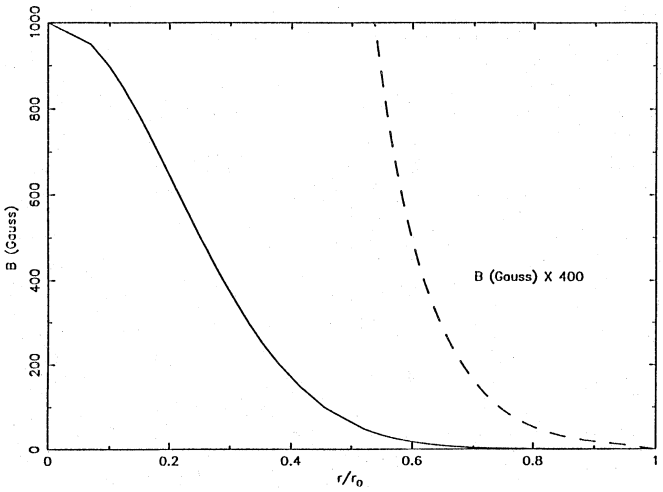

Fig. 1. Radial dependence of B_z the vertical component of the field

As shown in subsequent sections, pressure enhancements are generated in the flux tube that either slow down the inward radial velocity of neutrals or generate outward radial motions. The current generating layers are restrained to the ones where the radial velocity of neutrals is negative, corresponding to an inflow of angular momentum. This condition limits the vertical extension of the DC current generator.

3.3. Characteristics of the current system

The upper part of the ensemble of current generating layers will send (receive) currents predominantly into (from) the section of the circuit above it, since its resistance is lower than the resistance of the section below it. This conclusion reverses for the lower layers of this ensemble. Therefore, we expect the sign of the field aligned currents to change at some depth in the solar atmosphere. Similar conclusion holds in the model of current generation in a twisted magnetic field frozen in a plasma. In this case the maximum of the magnetic twist is usually assumed to be located at photospheric level, and currents above and below this level flow in opposite directions.

When the partial ionization of the plasma is taken into account, the height at which the vertical currents change of sign depends on the height dependence of the azimuthal velocity. In the numerical application presented here, where the azimuthal velocity at the periphery of the flux tube is constant and equal to 0.3 km s^{-1}, the change of sign occurs at a height of 200 km above the level where the continuum optical depth τ_{5000} is unity.

The radial currents are generated in low vertical magnetic fields. The radial current density amplitude shows a maximum and then decreases inwards. Accordingly the vertical currents must flow to neutralize the radial current. Two systems of vertical currents are then generated that flow in opposite directions.

These currents flow in two cylindrical shells near the boundary of the flux tube.

The characteristics of the system of currents have been computed for a flux tube of radius 100 km with a vertical magnetic field B_z on the vertical axis of the tube equal to 1000 Gauss and an azimuthal velocity of 0.3 km s^{-1} at the boundary. The radial variation of the vertical component of the magnetic field B_z is plotted in Fig. 1. Figs. 2a,b show the radial dependence of the radial and vertical current densities j_r and j_z at the altitudes of -25 and 50 km above $\tau_{5000} = 1$, and Fig. 2c gives j_z at the altitudes of 150 and 350 km.

4. Effects of the currents in the photosphere

Without radial and vertical currents, the dependence of the radial velocity would be linear in the photosphere. However, the electromagnetic forces generated by the currents modify the $V_{r,n}(r)$ law, and at a height of 350 km the radial velocity of neutral changes of sign and stops the influx of angular momentum. Consequently, the layers at 350 km and above cannot act as current generator and the radial current density j_r is null at $z = 350$ km.

The radial currents are generated near the boundary of the flux tube in low B_z field regions as it can be seen by comparison of Figs. 2a,b,c with Fig. 1. The vertical current density j_z profile shows a negative and a positive peak indicating the presence of two cylindrical shells of currents flowing in opposite directions. In each shell, the vertical current density j_z changes of sign at about 200 km, as shown on Fig. 2c. As it can be seen in Fig. 2d, since the two cylindrical shells of current flowing in opposite directions are generating repulsive forces they create a depression between them. On the other hand, the most internal current shell of current produces a pinch effect and increases the gas pressure inside the flux tube.

4.1. Photospheric upflows inside the internal current shell

In the flux tube the pressure enhancement due to the internal current shell reaches 10 % and it can generate upward flows and modify consequently the pressure of the upper atmospheric layers. The amplitude of the upflow can be estimated by solving the system of fluid dynamics equations for vertical motions in presence of some local overpressure δp

$$\rho \frac{d V_z}{dt} = -\frac{\partial}{\partial z}(p^\star + \delta p) - \rho\, g\,, \tag{13}$$

$$0 = -\frac{\partial p^\star}{\partial z} - \rho^\star\, g\,. \tag{14}$$

Here z is the altitude in the solar atmosphere, and $p^\star$ and $\rho^\star$ are the pressure and density corresponding to hydrostatic equilibrium. Then we assume steady state ($\partial V_z/\partial t = 0$) and no density changes, i.e. $\rho^\star = \rho$.

The equations (13) and (14) lead to

$$\frac{1}{2}\frac{\partial}{\partial z}\left(V_z^2\right) = g\,\left(\frac{\delta p}{p^\star}\right) - \frac{KT}{1.4 m_H}\frac{\partial}{\partial z}\left(\frac{\delta p}{p^\star}\right). \tag{15}$$

This equation is independent of density. Using the numerical expression of its coefficients at an altitude of about 50 km we obtain

$$\frac{\partial}{\partial z}\left(V_z^2\right) = 5.5 \times 10^4 \left(\frac{\delta p}{p^\star}\right) - 10^{12}\,\frac{\partial}{\partial z}\left(\frac{\delta p}{p^\star}\right). \tag{16}$$

At the height of 50 km, the relative pressure increase is $\delta p/p^\star \approx 0.1$, and in the photospheric layers the vertical gradient $\partial(\delta p/p^\star)/\partial z$ of the relative pressure increase is negative or null. A lower limit of the vertical velocity gradient is found for a null value of this gradient. This limit is

$$\frac{\partial}{\partial z}(V_z^2) = 5.5 \times 10^3 \text{ cm s}^{-2}.$$

Consequently, assuming a constant value of $\delta p/p^\star$, up to the height where the electric current goes through zero and changes of sign, i.e. over a vertical distance of 250 km, the vertical velocity can reach 3.5 km s^{-1}.

4.2. Upflows between the two current shells

Between the two current shells, the dominant force is the vertical $\mathbf{j}_r \times \mathbf{B}_\theta$ force. This force is directed upwards in the low photosphere and downwards in the upper photosphere where the sign of B_θ reverses. However, the dominant contribution comes from the denser lower photospheric layers. The velocity gradient is such that

$$\rho v_z \frac{\partial}{\partial z}(v_z) = j_r\, B_\theta - \rho g - \frac{\partial P}{\partial z}, \tag{17}$$

where ρ is the density. Assuming that the density ρ is equal to $\rho^\star$ the density in the hydrostatic atmosphere, equation (17) simplifies as

$$\rho v_z \frac{\partial}{\partial z}(v_z) = j_r\, B_\theta. \tag{18}$$

At $z = 0$ km, $j_r\, B_\theta$ reaches 6×10^{-2} Newton. This force is nearly equal to the gravity force. Consequently, a significant velocity gradient is present and

$$\frac{\partial}{\partial z}(V_z^2) = 5 \times 10^4 \quad \text{cm s}^{-2}.$$

In the hypothesis of constant density, a vertical velocity of about 7 km s^{-1} is reached over a vertical distance of 100 km. In order to explain the acceleration of spicules, the electromagnetic force $j_r\, B_\theta$ must lead to velocities of about 60 km s^{-1} at their base in order to rise matter to a height of about 7000 km. These velocities can be achieved since velocities in the 40 to 60 km s^{-1} range can be reached at the top of the photosphere since the density decreases with height by nearly two orders of magnitude.

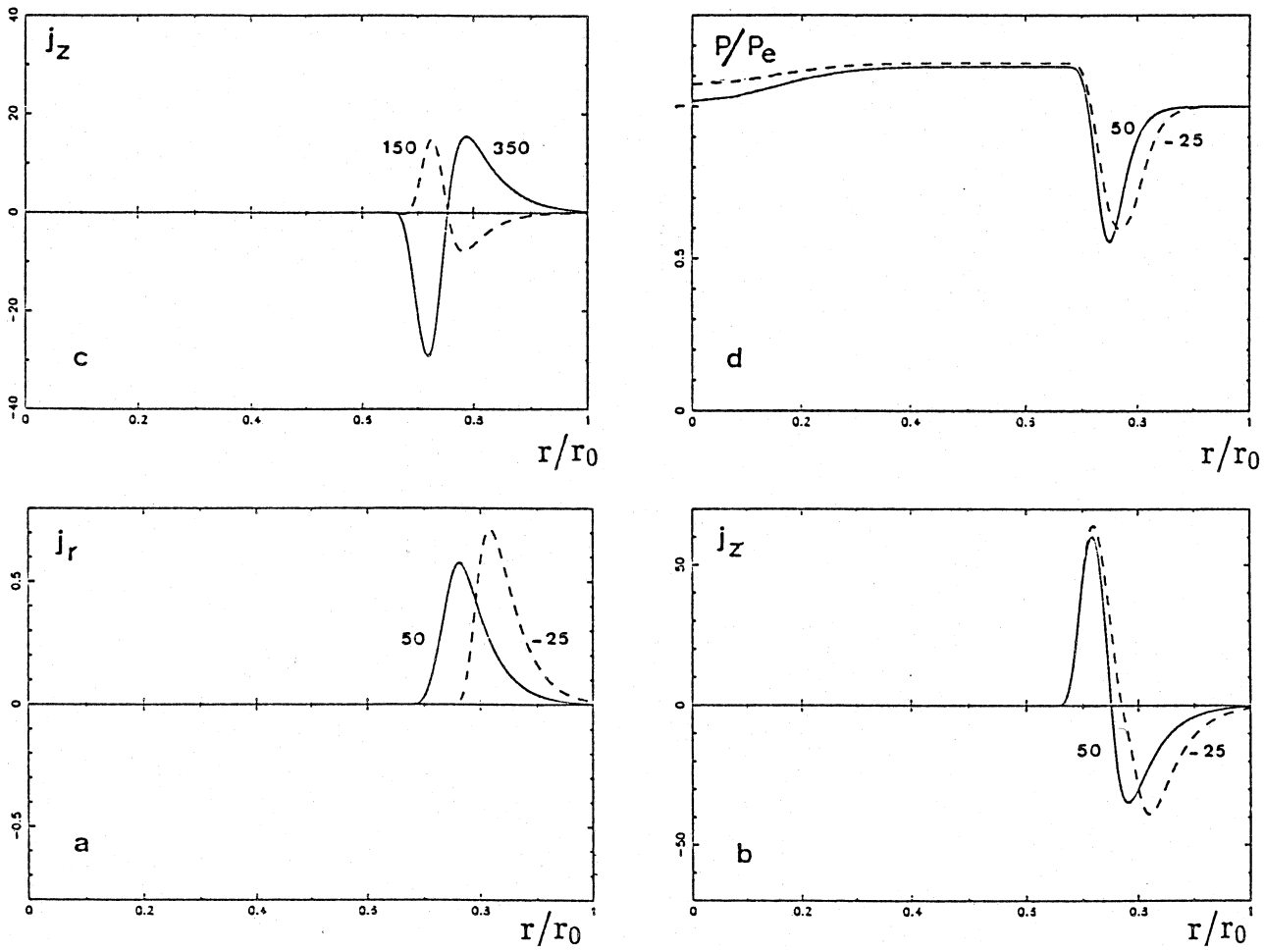

Fig. 2a–d. Radial dependence of: **a** - j_r the radial current density (Ampère m^{-2}), **b** and **c** - j_z (Ampère m^{-2}) the vertical current density, **d** - $p(r)/p(r_0)$ the ratio of gas pressure, at the depths of -25 and 50 km (**a, b, d**) and 150 and 350 km (**c**) above the level $\tau_{5000} = 1$ in the VAL C atmosphere.

5. Effects of the currents at chromospheric heights

The horizontal force balance equation can be written as

$$\frac{\partial p}{\partial r} + \frac{1}{2\mu}\frac{\partial B_z^2}{\partial r} + \frac{\mu}{8\pi^2 r^2}\frac{\partial J_z^2}{\partial r} = 0\,. \tag{19}$$

The third term on the LHS of Eq. (19) gives the $j_z B_\theta$ force. The direction of this force changes between the two vertical current systems.

At the boundary of the flux tube in the external DC current shell, the radial component of the electromagnetic force is directed outwards and can be compensated only by a pressure gradient. The resulting minimum of pressure $p_{\min}$ between the two current systems is approximatly equal to

$$p_{ext} - \frac{\mu}{8\pi^2}\frac{(J_z^{\max})^2}{r_0^2}\,, \tag{20}$$

where p_{ext} and $J_z^{\max}$ are the external pressure and the maximum value of the total vertical current J_z. Consequently the external cylindrical current system must open and increase in diameter in order to reduce the amplitude of the outward electromagnetic $j_z B_\theta$ force.

In the internal current shell, the $j_z B_\theta$ force is directed inwards. By pinch effect, this force can maintain a strong vertical magnetic field at the center of the flux tube, evoiding its opening with height and allowing a thin, nearly constant cross section, flux tube to extend into the chromosphere. Integrating Eq. (19) from the axis of the flux tube to the location where the current J_z is maximum leads to

$$\frac{\mu}{8\pi^2}\left(\frac{J_z^{\max}}{r_{\max}}\right)^2 = \left[\int_0^1 \frac{B_z^2(x)}{2\mu}\,dx^2 + \int_0^1 p(x)\,dx^2 - p_e\right]. \tag{21}$$

Here $r_{\max}$ is the radial distance at which J_z is maximum, p_e is the external pressure and $x = r/r_{\max}$. The magnetic field at the boundary of the flux tube is assumed to be negligible.

For low pressure forces, the magnetic field structure is force-free, corresponding to a balance between the energy stored in the vertical and azimuthal components of the field. The first term on the RHS of Eq. (21) represents the energy of the vertical component and, since the magnetic flux is constant, is propor-

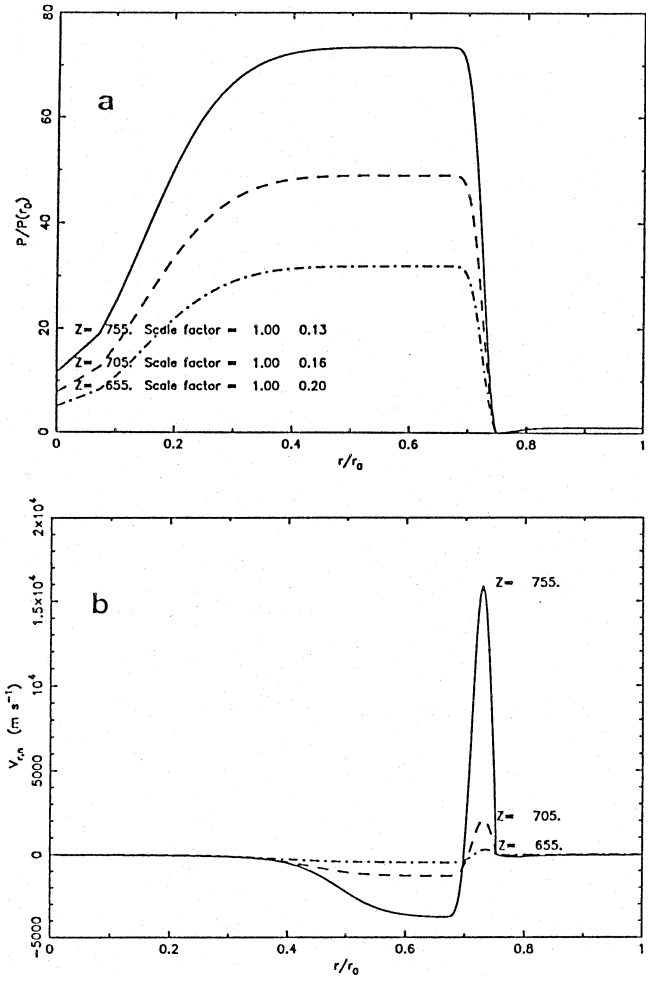

Fig. 3a and b. Radial dependence at three heights in the atmosphere, respectively 655, 705, and 755 km, for a flux tube of radius 100 km with an azimuthal velocity of neutrals at its boundary of 300 m s^{-1} of respectively: **a** - $p/p(r_0)$ the ratio of the local gas pressure to the external gas pressure, **b** - $V_{r,n}$ the radial velocity of neutrals. For each height, the two scale factor values give the inverse of the required increase of the radius of the internal and external cylindrical currents required for having a positive gas pressure at center and between the two currents shells.

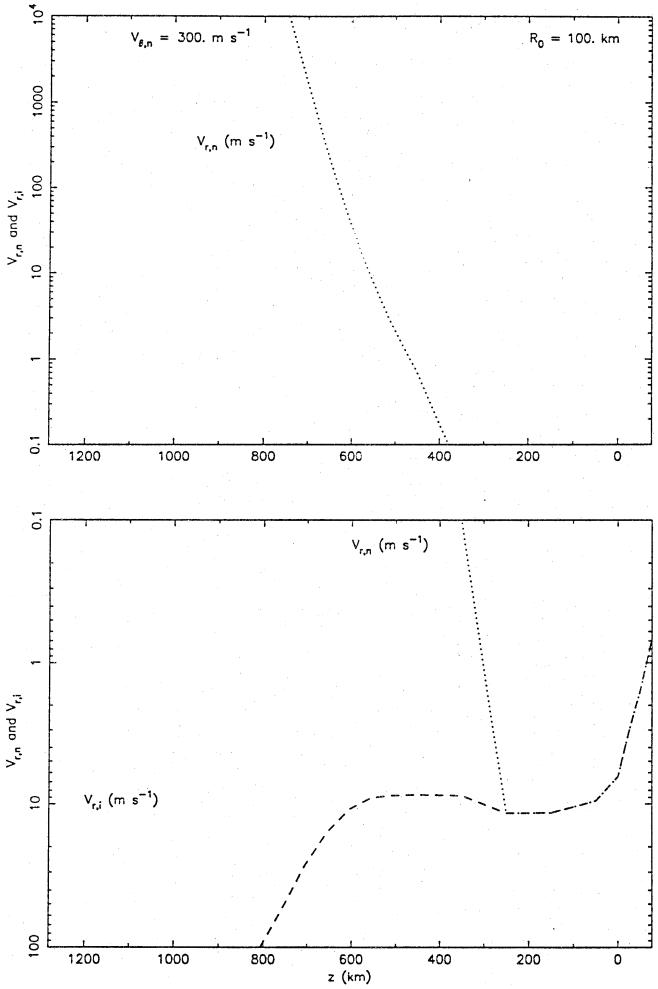

Fig. 4. Vertical dependence of the maxima of the radial velocities of neutrals (dotted line) and ions (dashed line).

tional to $1/r^2_{\rm max}$. Then, for a constant maximum current $J_z^{\rm max}$, if plasma is injected from the photosphere into the chromospheric part of a magnetic flux tube increasing the gas pressure, the tube must widen in order to reduce this first term. The equilibrium size of the flux tube will depend on the gas pressure, which is dependent on the flux and ionization state of the gas injected in the tube since, as discussed below, the non-ionized fraction of the plasma can escape across magnetic field lines.

For a prescribed radial dimension of the internal current shell, the radial dependence of pressure necessary to satisfy the force balance equation is shown in Fig. 3a at three heights in the chromosphere. This figure corresponds to a flux tube of 100 km radius with an azimuthal velocity of neutrals high enough to generate a vertical current that could confine a 1000 G field in a force-free situation. The radius corresponding to the force-free solution is proportional to the current intensity J_z:

$$r_c = \mu\, J_z \left[2\pi \left(\int_0^1 B_z^2/\mu x dx \right)^{1/2} \right]^{-1} . \qquad (22)$$

With the boundaries conditions used here (i.e. $B_z(0)$ = 1000 G and V_θ = 0.3 km s^{-1}), the radial dimension r_c is less than 100 km. Therefore, as illustrated in Fig. 3a, for these boundary conditions a significant pressure must be present in the tube to enlarge it to a radial size of 100 km.

Then the high pressure gradient required to balance the $j_z B_\theta$ force leads to a high speed radial outflow of neutrals as shown in Fig. 3b. This flow of neutrals across lines of force is possible since the densities are small enough for ions and neutrals not being coupled by collisions. The height dependence of the maxima of outward radial velocities of neutrals, when present, and of the inward velocities of ions and neutrals at the same radial distance are represented in Fig. 4. In the photosphere, ions and neutrals are collisionaly coupled. Higher in the atmosphere,

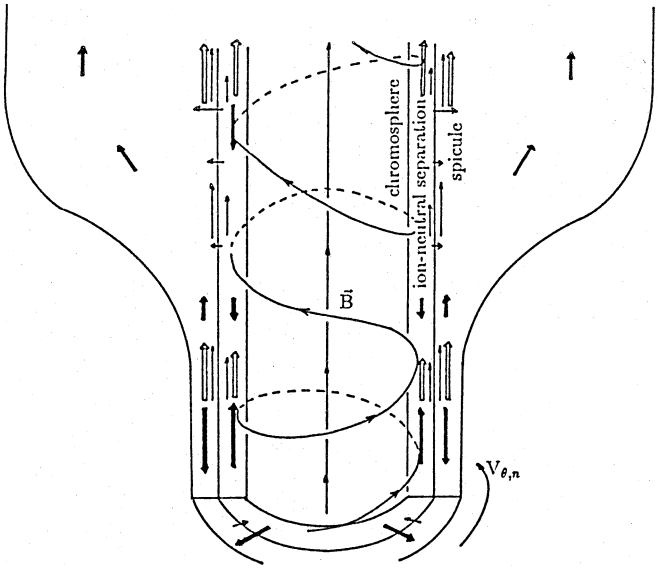

Fig. 5. Cut of the current shells near the external boundary of an open flux tube. Thick arrows: DC current; thin arrows: velocity of neutrals (high FIP elements); double thin line arrows: velocities of ions (low FIP elements). Spicules rise between the two current shells and ion-neutral separation takes place at the external border of the internal current shell contributing to the formation of a chromosphere. Notice the change with height of the sign of the azimuthal component of the magnetic field.

neutrals can move across the field lines. The reversal in the sign of the neutral radial velocity takes place around the temperature minimum region.

The situation described in the preceding section requires that a significant upflow of gas balances the escape of neutrals at chromospheric level. The upward velocity V_u is such that $V_u \approx V_r\,(\Delta r/\Delta z)\,(n_{ch}/n_{ph})$; where Δr is the radial extension of the photospheric pressure increase and Δz is the vertical extension of the chromospheric layer from which neutrals escape with a velocity V_r, and n_{ch}/n_{ph} is the ratio of chromospheric to photospheric densities of neutrals. An outflow at a velocity of 10 km s^{-1} over a depth of 50 km at a height of 800 km implies a moderate upflow $V_u \approx 2 \times 10^{-3}\ V_r \approx 20$ m s^{-1} compared to the upflow velocity found in Sect. 4.1. The consequences of the possible upflows and outflows of neutrals across lines of forces found in this Section and in Sect. 4 are examined below.

6. Discussion

A schematic representation of an open flux tube is given in Fig. 5, which shows the location and direction of the radial and vertical currents and the motions of the fluids of neutrals and ions. Excluding here the heating that currents can produce (Hirayama, 1992), three main effects of the electromagnetic forces generated by DC currents flowing in this flux tube can be distinguished, i.e. coronal abundance anomalies, formation of chromospheres, spicule acceleration.

6.1. Coronal abundance anomalies

Composition observations in the photosphere, upper transition region and corona, imply a change of composition of the solar atmosphere somewhere above the photosphere. The most prominent feature is an enrichment of elements with a low First Ionization Potential (FIP) relative to elements of high FIP. The process leading to such separation is estimated to operate at temperatures $T \approx 7000$ K (Meyer 1989).

The several possible mechanisms that could lead to neutrals-ions separation are reviewed in Meyer (1988, 1993a, 1993b), Von Steiger and Geiss (1989) and in Feldman (1992). Most models are based on the ion-atom separation occuring across magnetic field lines. For example, the gas could be driven across the field either by gravity (Vauclair and Meyer, 1985) or by a density gradient (Von Steiger and Geiss, 1989). The last authors considered a slab, parallel to an uniform magnetic field, filled with an initially neutral gas mixture. They looked at the evolution of the gas composition under the effect of diffusion across magnetic field lines and of photoionizing UV radiation. Their conclusion was that the leakage, out of narrow magnetic field structures, of atoms not yet ionized leads to ion-atom separation and to an overabundance of elements with low FIP in the ionized gas that is fed into the corona.

As pointed out in Hénoux and Somov (1992), forced diffusion across magnetic field lines and lift of the plasma to the corona are the necessary ingredients for any model of FIP fractionation. The most quantitative work on coronal abundance anomaly was published by Von Steiger and Geiss (1989) and it was based on ion-neutral separation in a gas injected as a pressure pulse in a magnetic field. Such conditions occur naturally in the current carrying flux tubes considered in our model and the ion neutral separation takes place at the right place, i.e. in the chromosphere: due to the pinch effect in the photosphere produced by the internal current shell, the partially ionized photospheric plasma rises into the flux tube and is depleted at chromospheric level in neutral high FIP elements. Consequently the gas inside the inside the internal current shell is enriched in low FIP elements in the chromosphere and above.

The possibility to detect the resulting change in abundances are presumably limited to the coronal level since at chromospheric level the internal current shell depleted in high FIP will be surrounded by the high FIP elements ejected between the two current shell. There must be a lower limit of the height at which the enrichment is high enough for the effect to be detectable and not compensated by the effects of the surrounding. Indeed such model is still qualitative, and a quantitative study must be done that would include a precise study of the ionization equilibrium taking into account ionization, recombination and radiative transfer processes.

6.2. Formation of chromospheres

Decoupling between ions and neutrals takes place at chromospheric heights and starts around the temperature minimum level. This suggests that the chromosphere – defined as a rise

of the ionization degree with height – could result from the ion-neutral separation in concentrated magnetic flux tubes.

It can be shown that the degree of ionization rises with height. Considering a flux-tube slab of thickness Δh, the increase of the ion density number per unit of time, inside this slab, due to an upflow at velocity V_z of ions and neutrals is

$$\frac{dn_i}{dt} = \frac{n_n x_i \Delta V_z}{\Delta h}. \tag{23}$$

Where x_i is the degree of ionization. Assuming that the net flux of neutrals inside the slab is null, $\Delta V_z = 2\,V_{r,n}\Delta h/r$ and

$$\frac{dn_i}{dt} = \frac{2\,n_n x_i V_{r,n}}{r}, \qquad \text{giving} \qquad x_i = x_{i,0}\exp\,(t/\tau), \tag{24}$$

where $\tau = r/2V_{r,n}$. Indeed an accurate computation of the degree of ionization inside the flux-tube has to include the effect of recombination and photoionization. This is outside the scope of our paper. However, Eq. (24) shows that, even if the final temperature and density distribution is not accurately determined, electromagnetic separation between ions and neutrals enhances the ion population and that this effect increases with height. Consequently, the degree of ionization is expected also to increase with height, and a rise of the degree of ionization and of the temperature with height is a typical characteristic of chromospheres.

According to our model, energy can be brought into the chromosphere as ionization energy carried by ionized low FIP elements. The energy flux into the chromosphere in the internal current shell is then $F = \overline{\chi_l n_l}\,V_{up}$, where $\overline{\chi_l n_l}$ is the mean value of the product of χ_l, the ionization potential, by n_l, the number density of low FIP elements. Taking $\overline{\chi_l n_l} = 7.8$ eV$\times 10^{13}$ cm^{-3} the energy flux required to heat the chromosphere is obtained for upflow velocities $V_{up} \approx 300$ m s^{-1} at photospheric level. Such velocity is low compared to the so called macro-turbulence used to explain photospheric line profiles and can be generated by pinch effect as discussed in Sect. 4.1. It was shown in this section that velocities of the order of 3.5 km s^{-1} can be generated. Since the pressure increase due to pinch is limited to the periphery of the internal current, i.e. in about one tenth of the flux tube cross section area, the mean velocity is well in the 300 m s^{-1} velocity range. This despite the slow downward motions of a few m s^{-1} that take place in the low gas pressure part of the flux tube near it axis of symetry, as a result of slow motions transverse to the magnetic field (see Paper I).

Consequently, as suggested by observations (e.g. Ayres, 1989; Kozlova and Somov, 1995), the upper part of the atmosphere becomes structured in cool non-magnetic regions and magnetic hot "bright points". The last can be enriched in elements of low FIP. To the contrary, in the lower part of the photosphere, magnetic points are cooler than the surroundings.

In fact, Ayres and Testerman (1981), Ayres *et al*. (1986), Ayres and Wiedeman (1989) assumed the existence of a highly thermically structured atmosphere in order to explain the low brightness temperature of the strongest CO lines (Noyes and Hall, 1972; Ayres and Testerman, 1981). The upper atmosphere would contain substantial amount of cool material in addition to hot gas ($T > 6000$ K). Less than 10% of the atmosphere in quiet regions and about 50% in magnetic active regions would contain chromospheric hot gas. The chromospheric temperature inversion would take place only in hot regions.

The need for a thermal structured atmosphere also comes from the impossibility to get energy balance at the temperature minimum and in the low chromosphere with an horizontally homogeneous model of the quiet sun. With such model, H^-, that dominates the total net rate of radiative cooling, is a net radiative heating agent (Vernazza *et al*. 1981; Avrett 1985), and the CO cooling is not a sufficient cooling agent to compensate for the energy deposite (Mauas *et al*. 1989).

Therefore, the thermally structured model of the atmosphere was observationally well justified, but its origin was never clearly understood. The coexistence of cold and hot components in the high atmosphere was attributed by Ayres and Testerman (1981) to a thermal instability driven by an assumed very powerfull cooling in the CO bands. The creation by cooling of CO molecules would enhance the cooling in low-temperature regions untill all the carbon is in CO molecules. A different conclusion was, however, reached by Mauas *et al*. (1989). They found that in the temperature range 3700–4700 K the CO cooling rate is insufficient to cancel the negative H^- heating rate. These authors also ruled out the possibility of CO cooling to be responsible for the existence of the cool gas.

Our computations show that due to the difference in the velocities of neutrals and ions across the magnetic field lines:

1. Neutrals are injected into non-magnetic regions, but ions fill magnetic "bright points", creating a structure separated into regions of high and low degree of ionization.
2. Hot regions are associated with thin magnetic flux tubes and cool gas with non-magnetic regions, as was presumed but not explained in the empirical model by Ayres.
3. The electric current required to maintain a pressure excess in the upper part of the flux tube can be generated in the photosphere.

Therefore, we propose that the thermal structure of the chromosphere and the chromospheric temperature inversion take place inside thin magnetic flux tubes.

6.3. Spicules

In open magnetic flux tubes, in the low pressure region between the two current shells, the $j_z B_\theta$ force can accelerate the plasma to high velocities in the chromosphere. Since the plasma motion is not slow down by pinch effects in the chromosphere, these velocities are high enough for the plasma to reach the altitude of about 7000 km reached by spicules, Hirayama (1992) suggested a possible rôle of Joule heating on spicule formation. We think that the $j_r\,B_\theta$ electromagnetic force is the best candidate to explain spicule formation. The amplitudes of the upward force and of the upward velocity depend on the flux tube radius and on the azimuthal velocity at the periphery of the tube. Since the values used in this study are moderate, higher values can be used,

and there is no doubt that the inflow of angular momentum into flux tubes can generate the required high upwards velocities for spicule formation. However, since spicules are transitory phenomena, the $j_r\, B_\theta$ force must have a transitory character. This may come naturally from the transitory character of the azimuthal velocities.

7. Conclusions

The consideration of the motion of each the three fluids made of neutrals, ions and electrons, is not simple but leads to a physical description of the formation and structure of thin magnetic flux tubes (see also Paper I) that explains several observational facts:

1. At deep photospheric levels, flux tubes are presumably cooler than their surroundings.
2. In the chromosphere, above the temperature minimum region, flux tubes are presumably hotter than surroundings.
3. The coronal abundances of elements are different from the photospheric abundances and depend on the FIP.
4. Matter is ejected with high upwards velocities in spicules.

It is worth noticing that electric currents in flux tubes explain at least qualitatively these four items including both the formation of the solar chromosphere, coronal abondance anomalies and spicules generation. The first item was treated in paper I. The second and third item result from the possible fast outflow of neutrals across the lines of force, that leads to a separation between highly ionized magnetic flux-tubes, enriched in elements of low first ionization potential, and a more extended region with a weaker degree of ionization and therefore with a lower temperature. Our model indicates also that plasma must be ejected to high altitude like as observed in spicules. Consequently, electric currents play a significant rôle in the physics of thin flux tubes that cannot be treated without taking into account the not small deviation from ideal MHD.

Appendix A: complete expressions of the ions and neutrals velocities

In Hénoux and Somov (1991), velocities of electrons, ions and neutrals have been computed, for an axially symmetrical magnetic field, in the three fluids approximation, by solving the equations that express the balance of the horizontal forces acting per unit volume on each particle fluid, i.e.

$$n_k \textstyle\sum_l \boldsymbol{F}_{l,k} + q_k n_k(\boldsymbol{V}_k - \boldsymbol{V}^c) \wedge \boldsymbol{B_z} - \boldsymbol{\nabla} P_k + q_k n_k(\boldsymbol{V}_{z,k} - \boldsymbol{V}^c_z) \wedge \boldsymbol{B} = n_k m_k \boldsymbol{V}_k.\boldsymbol{\nabla} V_k. \quad \text{(A1)}$$

Here $\boldsymbol{F}_{l,k}$ is the friction force due to particles l acting on a particule k, and $\boldsymbol{F}_{l,k} = m_k \nu_{kl}(\boldsymbol{V}_l - \boldsymbol{V}_k)$. $\boldsymbol{B}$ and $\boldsymbol{E}$ are the magnetic and electric field vectors. $\boldsymbol{V}_k$, n_k and m_k are the drift velocity, density and mass of a particle k. ν_{kl} is the coefficient of friction between particles k and l. $\boldsymbol{V}^c$ is the velocity field in the convective zone.

The horizontal velocities of ions and neutrals derived from the equations above are (Hénoux and Somov, 1991):

$$V_{r,i} = -f(\nu)\frac{j_\theta B_z}{n_e} + V_{z,i}\frac{B_r}{B_z} + I_{r,i}, \quad \text{(A2)}$$

$$V_{\theta,i} = -f(\nu)\frac{j_z B_r}{n_e} + \frac{1}{e n_e B_z}\left(\frac{\partial P_i^\star}{\partial r} + n_e \frac{m_i \nu_i}{\alpha_s}\frac{\partial P_n^\star}{\partial r}\right) + V_{z,i}\frac{B_\theta}{B_z} + I_{\theta,i}, \quad \text{(A3)}$$

$$V_{r,n} = -f(\nu)\frac{j_\theta B_z}{n_e} + n_e \frac{[m_i\nu_i V_{z,i} + m_e \nu_e V_{z,e}]B_r}{\alpha_s B_z} - \frac{1}{\alpha_s}\frac{\partial P_n^\star}{\partial r} + I_{r,n}, \quad \text{(A4)}$$

$$V_{\theta,n} = -f(\nu)\frac{j_z B_r}{n_e} + \frac{1}{e B_z}\left(\frac{\partial P_i^\star}{\partial r} + \frac{\partial P_n^\star}{\partial r}\right)\left(\frac{m_i\nu_i - m_e\nu_e}{\alpha_s}\right) + n_e \frac{[m_i\nu_i V_{z,i} + m_e\nu_e V_{z,e}]}{\alpha_s}\frac{B_\theta}{B_z} + I_{\theta,n}\,. \quad \text{(A5)}$$

The ions and neutrals velocities in these equations are relatives to the velocities in the convective zone, since all components of the vector $\boldsymbol{V}_k - \boldsymbol{V}^c$ have been replaced by $\boldsymbol{V}_k$. The function $f(\nu)$ is given by:

$$f(\nu) = \frac{1}{e^2 B_z^2}\left[\frac{m_e\nu_e m_i \nu_i}{(m_e\nu_e + m_i\nu_i)} + m_e \nu_{ei}\right] = \frac{n_e}{B_z^2 \sigma}, \quad \text{(A6)}$$

where σ is the electric conductivity parallel to $\boldsymbol{B}$. $\alpha_s = n_e(m_i\nu_i + m_e\nu_e)\,\nu_e$ where ν_i and ν_{ei} are the collision frequencies between electrons, ions and neutrals and between electrons and ions. $I_{r,k}$ and $I_{\theta,k}$ are the contributions to $V_{r,k}$ and $V_{\theta,k}$ of the inertial terms. They are given by:

$$I_{r,i} = -\frac{n_i m_i V_{r,i}}{n_e e B_z r}\frac{\partial(rV_{\theta,i})}{\partial r} - \frac{n_n m_n}{e B_z}\frac{m_i\nu_i}{\alpha_s}\frac{V_{r,n}}{r}\frac{\partial(rV_{\theta,n})}{\partial r}, \quad \text{(A7)}$$

$$I_{\theta,i} = -f(\nu)\frac{1}{r n_e}\sum_k n_k m_k V_{r,k}\frac{\partial(rV_{\theta,k})}{\partial r}, \quad \text{(A8)}$$

$$I_{r,n} = -\frac{n_e}{r e B_z \alpha_s}[\nu_i {m_i}^2 V_{r,i}\frac{\partial(rV_{\theta,i})}{\partial r} - \nu_e {m_e}^2 V_{r,e}\frac{\partial(rV_{\theta,e})}{\partial r} + \frac{(m_e\nu_e)^2 + (m_i\nu_i)^2}{\alpha_s} n_n m_n V_{r,n}\frac{\partial(rV_{\theta,n})}{\partial r}], \quad \text{(A9)}$$

$$I_{\theta,n} = -f(\nu)\frac{1}{r n_e}\sum_k n_k m_k V_{r,k}\frac{\partial(rV_{\theta,k})}{\partial r} - \frac{n_n m_n}{\alpha_s}\frac{V_{r,n}}{r}\frac{\partial(rV_{\theta,n})}{\partial r}. \quad \text{(A10)}$$

The summation is made over all species, electrons, ions and neutrals. The azimuthal and radial current densities are found to be

$$j_\theta = (j_z B_\theta + \frac{\partial P^\star}{\partial r})/B_z = -\frac{1}{\mu}\frac{\partial B_z}{\partial r}, \quad \text{(A11)}$$

$$j_r = \frac{1}{B_z}\left(j_z B_r - \frac{1}{r}\sum_k n_k m_k V_{r,k}\frac{\partial(rV_{\theta,k})}{\partial r}\right), \quad \text{(A12)}$$

where j_z is the vertical current density. $P^\star$ is defined by $P^\star = \sum_k P_k^\star$ where $P_k^\star$ is defined by :

$$\frac{\partial P_k^\star}{\partial r} = \frac{\partial P_k}{\partial r} + \frac{1}{2} n_k m_k \frac{V_{r,k}^2}{\partial r} - \frac{1}{r} V_{\theta,k}^2. \quad \text{(A13)}$$

The subscripts θ, r, z refer to the azimuthal, radial and vertical components of the magnetic and velocity fields. The subscripts i, e and n correspond respectively to the ions, electrons, and neutrals.

The equation (A.11) can be rewritten as

$$\frac{\partial P^\star}{\partial r} = -\frac{1}{2\mu}\left(\frac{\mu^2}{4\,\pi^2 r^2}\frac{\partial J_z^2}{\partial r} + \frac{\partial B_z^2}{\partial r}\right) \quad \text{(A14)}$$

Appendix B: radial velocities of ions and neutrals

Assuming no radial motions in the convective zone and that the radial component of $\boldsymbol{B}$ is null, we can write the radial velocities of neutrals and ions as :

$$V_{r,i} = -\frac{j_\theta B_z}{\sigma B_z^2} + I_{r,i} = \frac{1}{2\mu\sigma B_z^2}\frac{\partial B_z^2}{\partial r} + I_{r,i}, \quad \text{(B1)}$$

$$V_{r,n} = V_{r,i} - \frac{1}{\alpha_s}\frac{\partial P_n^\star}{\partial r}. \quad \text{(B2)}$$

Neglecting the contribution of electrons and in the hypothesis that $B_r = 0$, we obtain from equations (A.7) and (A.12) $I_{r,i} \simeq j_r/n_e e$. Consequently the radial velocities of ions and neutrals are given by

$$V_{r,i} = \frac{1}{2\mu\sigma B_z^2}\frac{\partial B_z^2}{\partial r} + \frac{j_r}{n_e e},, \quad \text{(B3)}$$

$$V_{r,n} = \frac{1}{2\mu\alpha_s}\left(\frac{\partial B_z^2}{\partial r}(1 + \frac{\alpha_s}{\sigma B_z^2}) + \frac{\mu^2}{4\pi^2 r^2}\frac{\partial J_z^2}{\partial r}\right) + \frac{j_r}{n_e e}. \quad \text{(B4)}$$

Appendix C: azimuthal velocity of neutrals

The radial dependence of $rV_{\theta,n}$ can be derived from equations (A.5) and (A.10). Considering successively the various terms on the RHS of eq.(A.5) we show below that the last term is the dominant term on the RHS of this equation. *i*) The third term, that is indeed null for a vertical magnetic field, gives the effect, on the azimuthal velocity of neutrals, of the collisions with charges, ions and electrons, moving along the lines of force. Since the velocities that neutrals achieve under the effect of these collisions are also parallel to the lines of force, they do not imply any electromagnetic force and the third term can be omitted. Ignoring this term implies that the azimuthal velocity in the LHS of the simplified resulting equation is the azimuthal component of the velocity vector component that is perpendicular to the magnetic field vector. *ii*) The second term gives the limit of the azimuthal velocity of neutrals, that does result from the collisions with the charged particles that carry the azimuthal current j_θ. In the region of generation of the radial currents. This velocity is orders of magnitude smaller that the azimuthal velocity of neutrals and can therefore be neglected. *iii*) In the thin flux-tube approximation the first term on the RHS is null. Then the azimuthal velocity of neutrals can be rewritten as

$$V_{\theta,n} \simeq -\frac{1}{r} n_n m_n V_{r,n}\left(\frac{1}{\alpha_s} + \frac{1}{B_z^2\sigma}\right)\frac{\partial r V_{\theta,n}}{\partial r}. \quad \text{(C1)}$$

References

Avrett, E.H. 1985, in *Chromospheric Diagnostics and Modelling*, Ed. B.W. Lites, Sunspot, N.M.: National Solar Observatory, p. 67

Ayres, T.R. 1989, in *Solar photosphere: structure, convection and magnetic field* , IAU Sympos. 138, Ed. J.O. Stenflo, Kluwer Academic Publishers, Dordrecht, p. 23

Ayres, T.R. and Testerman, L. 1981, ApJ 245, 1124

Ayres, T.R., Testerman, L., and Brault, J.W. 1986, ApJ 304, 542

Ayres, T.R. and Wiedeman, G.R. 1989, ApJ 338, 1033

Feldman, U. 1992, Phys. Scripta 46, 202

Hénoux, J.C. and Somov, B.V. 1991, A&A 241, 613

Hénoux, J.C. and Somov, B.V. 1992, in *Proc. of the First SOHO Workshop*, ESA SP-348, p. 325

Hénoux, J.C. and Somov, B.V. 1993, Adv. Space Res. 13, No. 9, 23

Hénoux, J.C. and Somov, B.V. 1994, in *Solar Active Region Evolution: Comparing Models with Observations*, Eds. K.S. Balasubrammaniam and G.W. Simon, ASP Conf. Series, Vol. 68, p. 158

Hirayama T. 1992, Solar Phys. 137, 33

Kozlova, L.M. and Somov, B.V. 1995, Bull. Russ. Acad. Sci., Physics 59, No. 7, 124

Kubát, J. and Karlický, M. 1986, Bull. Astron. Inst. Czechosl. 37, 155

Mauas, P.J., Avrett, E.H., and Loeser, R. 1989, ApJ 345, 1104

Meyer, J.P. 1988, in *Origin and Distribution of the Elements* Ed. G.E. Mathews, World Scientific, p. 310

Meyer, J.P. 1989, in *Cosmic Abundances of Matter* Ed. C.J. Waddington, New York: American Institute of Physics, p. 245

Meyer, J.P. 1993, Adv. Space Res., Vol.13, No. 9, 377

Meyer, J.P. 1993, in *Origin and Evolution of the Elements*, eds. N. Prantzos, E. Vangioni-Flam and M. Cassé, Cambridge Univ. Press. p.6

Noyes, R.W. and Hall, D.N.B. 1972, ApJ 176, L89

Steinolfsen, R.S. 1991, ApJ 382, 677

Somov, B.V., *Fundamentals of Cosmic Electrodynamics*, Kluwer Academic Publishers, Dordrecht, 1994.

Vauclair, S. and Meyer, J.P. 1985, in *19th Intern. Cosmic Ray Conf*. La Jolla, 4, 233

Vernazza, J.E., Avrett, E.H., and Loeser, R. 1981, ApJS 45, 635

Von Steiger, R. and Geiss, J.R. 1989, A&A 225, 222

This article was processed by the author using Springer-Verlag LaTeX A&A style file *L-AA* version 3.